CONSISTENCY OF ABOVE AND IN-WATER RADIOMETRIC MEASUREMENTS IN EUTROPHIC AND ABSORBING WATERS

Krista Alikas*[1], Peter Gege[2], Stefan Plattner[2], Ian Somlai-Schweiger[2], Kersti Kangro[1], Ave Ansper-Toomsalu[1], Nicole Pinnel[2], Ilmar Ansko[1], Riho Vendt[1]

[1]Tartu Observatory, Tartu University, Tõravere, Observatooriumi 1, 61602, Estonia
[2]Deutsches Zentrum für Luft- und Raumfahrt (DLR), Remote Sensing Technology Institute, Oberpfaffenhofen, 82234 Wessling, Germany
*Corresponding author: alikas@ut.ee

Deutsches Zentrum für Luft- und Raumfahrt German Aerospace Center

Estonian Research Council

UNIVERSITY OF TARTU

Radiometric measurements were conducted across nine optically complex lakes representing a wide range of conditions, from Nohipalu Valgjärv (Chl a = 1.6 µg/L, $a_{CDOM}(442)$ = 1.5 m^{-1}, TSM = 1 mg/L) to highly eutrophic and strongly absorbing lakes, with chlorophyll-a concentrations reaching up to 149 µg/l and aCDOM(442) up to 54 m–1.

Four sets of both above-water and in-water radiometric measurement setups were used across these lakes.

1. OOSS is a handheld spectrometer system stabilized with a gimbal for performing measurements from a boat or platform. Developed and built at DLR.
2. LimnoVIS is an unmanned surface vehicle (USV) for collecting hyperspectral in-situ data in inland waters. It can be operated either remotely or autonomously, maintaining the configured measurement position and orientation. Developed and built at DLR.
3. TriOS RAMSES above water set consisting of three sensors: $L_u(\lambda)$ is the upwelling radiance from the water, $L_d(\lambda)$ is the downwelling radiance from the sky, and $E_d(\lambda)$ is the downwelling irradiance
4. TriOS RAMSES in-water set consisting of two sensors: $L_u(\lambda)$ is the upwelling radiance from the water and $E_d(\lambda)$ is the downwelling irradiance.

The performance of the different setups, along with their associated interpolation schemes, was compared, and the consistency between above-water and in-water radiometric measurements was assessed.

Table 1. Description of different study sites and the measurement conditions

Lake	station_id	Sun	Date	Cloudiness	Wind speed	Secchi depth	Wave height	TSM (mg/L)	Chla (µg/L)	CDOM 443nm (m^{-1})
Võrtsjärv1	4335	Through thin cloud	2025-05-27	100	1	0.7	0.1	13.6	32.7	2.9
Võrtsjärv2	4336	Through thin cloud	2025-05-27	100	3	0.9	0.1	8.8	19.5	6.4
Võrtsjärv3	4337	Through thin cloud	2025-05-27	100	2.5	0.8	0.1	14	30.7	4
Võrtsjärv4	4338	Fully covered	2025-05-27	100	1	0.7	0.05	16.8	32.2	3.2
Nohipalu Valgjärv	4342	Through thin cloud	2025-05-28	100	0	3.2	0	1	2.3	1.5
Nohipalu Mustjärv	4343	Partially covered	2025-05-28	100	2	0.4	0	3.6	28.1	**54.3**
Tamula	4340	Clear	2025-05-30	80	4	1.3	0.15	3.6	2.7	2.1
Vagula	4339	Clear	2025-05-30	40	3	2	0.05	**28**	9.4	4
Saadjärv	4341	Clear	2025-06-01	90	5	4.8	0.15	1.5	5.6	1.2
Võnnu	4347	Through thin cloud	2025-06-04	50	3	0.4	0	**35.3**	**159.9**	3.3
Meelva	4345	Through thin cloud	2025-06-04	90	3	0.4	0.05	2.5	32.6	**51.4**
Verevi	4346	Through thin cloud	2025-06-04	70	3	2.5	0.05	3.2	3.7	3.5
Verevi2	4349	Through thin cloud	2025-06-04	80	3	2.5	0	3.2	3.7	3.5

Measurement procedure and data analyses

Both the OOSS and LimnoVIS measure upwelling radiance ($L_u(\lambda)$) of the water surface and a calibrated reflectance panel using a single field spectrometer each. Each dataset consists of 30 single measurements. The water Lu is measured at viewing angles of 30° and 40°, the panel at nadir. The dark background is subtracted from the measurements, and outliers are discarded to calculate the mean water and panel Lu spectra.
The panel $L_u(\lambda)$ spectrum is multiplied with π and divided by its calibrated reflectance spectrum to obtain the downwelling irradiance ($E_d(\lambda)$). The water radiance reflectance for both viewing angles is then calculated by dividing the water $L_u(\lambda)$ spectrum by the $E_d(\lambda)$ spectrum. Finally, the remote-sensing reflectance, $R_{rs}(\lambda)$, in units of sr^-1, is obtained by correcting the water's radiance reflectance for sun and sky glint using the software WASI (Gege, 2024).

TriOS RAMSES above water measurements were recorded for at least 10 min at each station. The $R_{rs}(\lambda)$ was calculated from the well-synchronized time series measured with the three above water TriOS-RAMSES hyperspectral radiometers. The data was processed with HyperCP processor by applying Zhang et al., 2017 sky and sunglint correction. 300 sec ensemble intervals were used from one station measurements.

TriOS RAMSES in-water measurements were performed with $L_u(\lambda)$ and $E_d(\lambda)$ sensors. Vertical profiles were measured at fixed depths, starting with a measurement above the water surface, followed by a measurement just below the water surface, and then measurements at 0.5 m depth intervals (0.5, 1.0, 1.5 m, etc.) until there was no measurable signal any more. Five measurements were performed at each depth.
At each depth, median values for $L_u(z,\lambda)$ were derived (Figure 1, Figure 2) and used to extrapolate $L_u(z,\lambda)$ to sub-surface $L_u(0-,\lambda)$. $L_u(0-,\lambda)$ was converted to $R_{rs}(\lambda)$ by applying the air–water transmission factor of 0.543 (Austin, 1974) and immersion factor; and dividing the $L_u(0^+,\lambda)$ spectrum by the above water measured $E_d(\lambda)$ spectrum.

Below water TRiOS RAMSES profiles for each study site

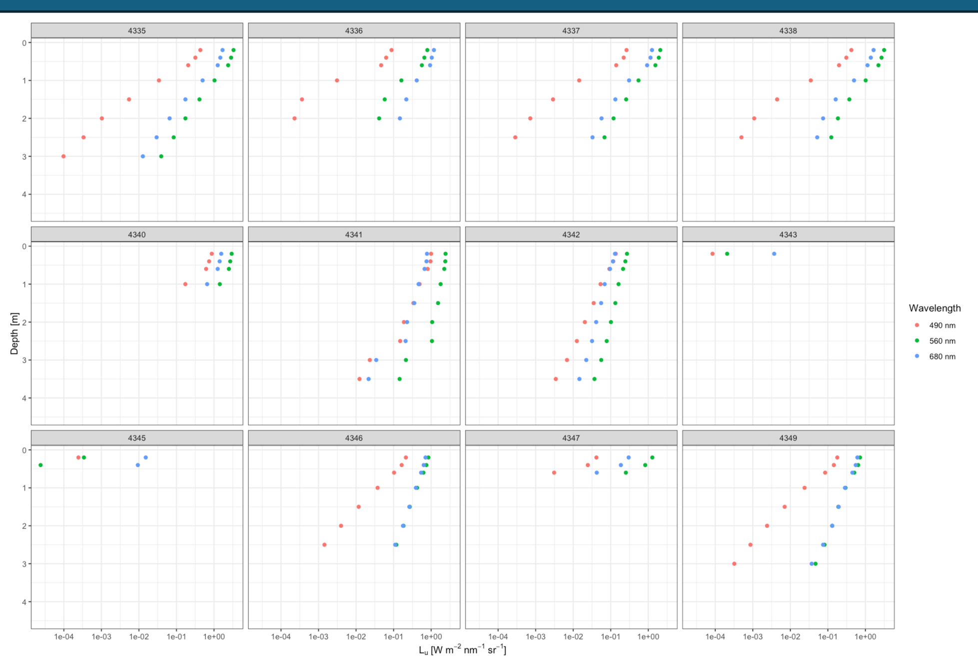

Figure 1. For highly absorbing (#4343, #4345) and highly eutrophic waters (#4347) only upper layer (0.4 and 0.6 m) is measurable.
Linearity of log-transformed radiometric profile data with depth depends on the measurement conditions and wavelength. In addition to perturbations by deployment structure, the near-surface radiance distribution may be affected by scattering, absorption, and wave-induced disturbances, as well as by inelastic processes such as Raman scattering and chlorophyll-a fluorescence.

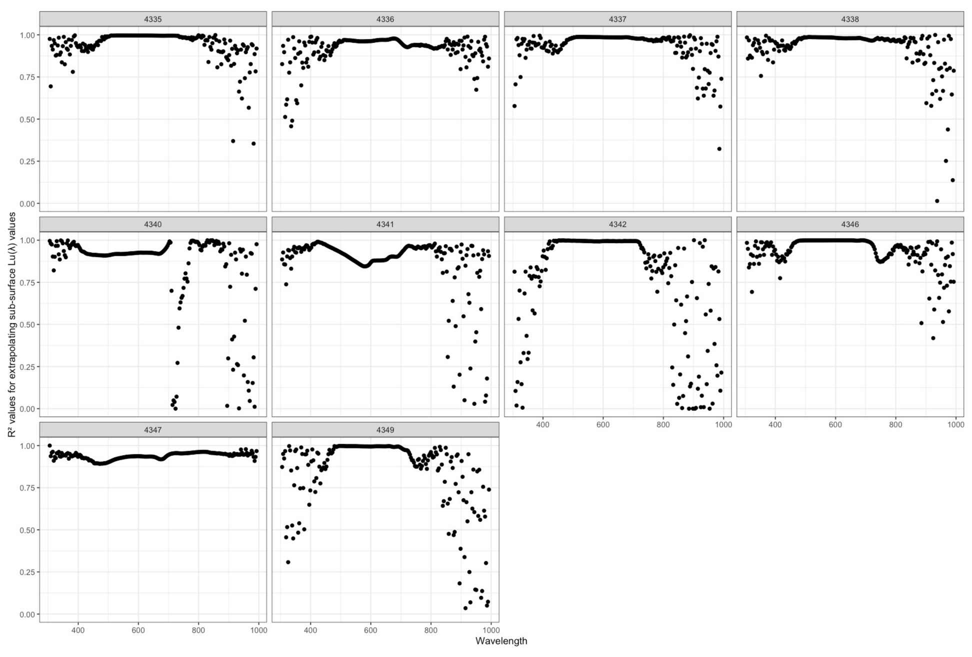

Figure 2. The coefficient of determination for extrapolating of sub-surface values

Consistency of above- and in-water TRiOS RAMSES radiometric measurements

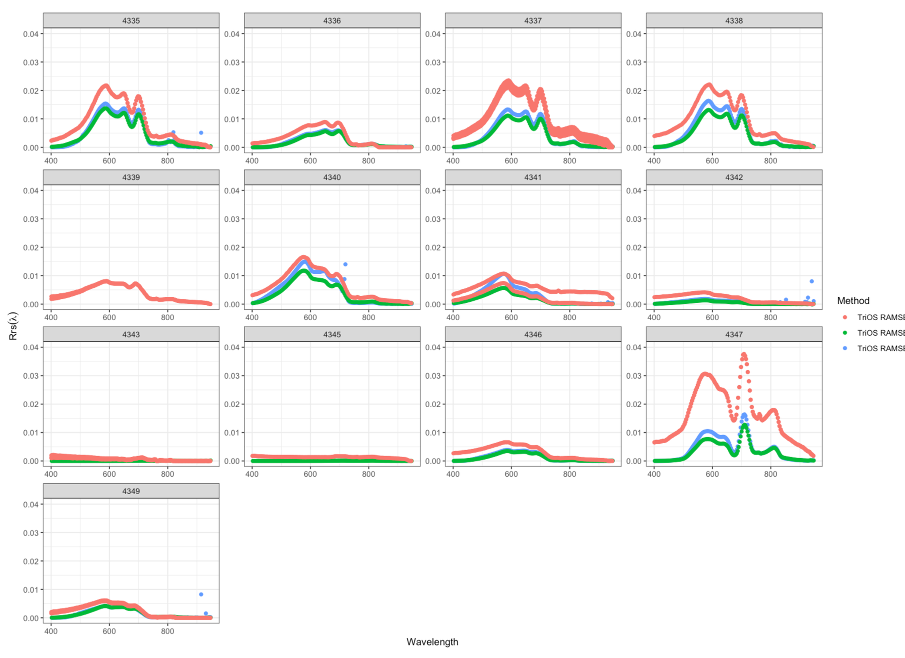

Figure 3. Comparison of above-water-derived reflectance (Rrs_hyper) with below-water measurements obtained from profiles (R2 profile) or at fixed depths (R2 below).

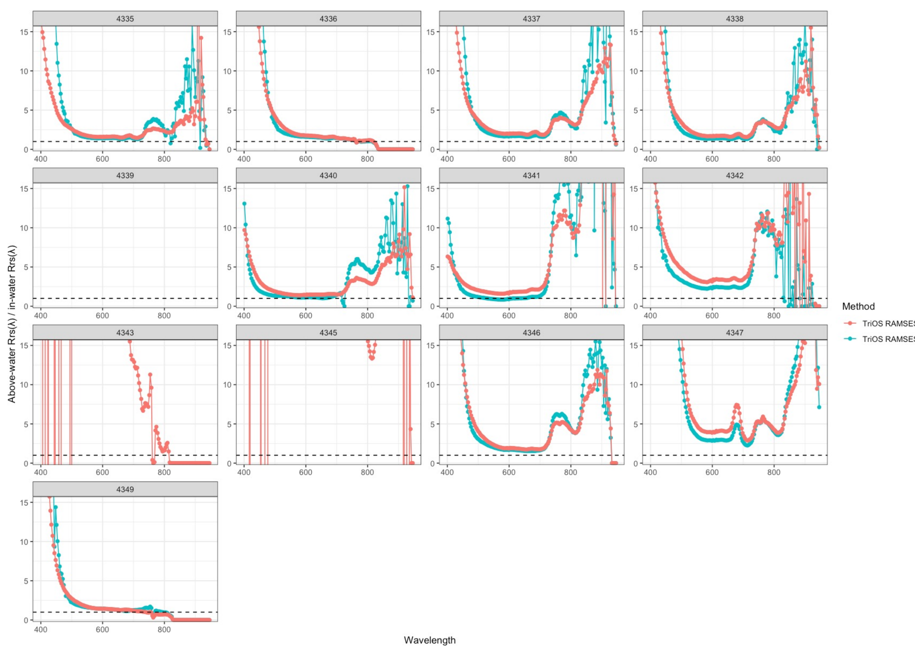

Figure 4. Ratios of above-water derived Rrs to below-water measurements from profiles (R2 profile) or fixed depths (R2 below) at each study site.

Comparison of above- and in-water TRiOS RAMSES radiometric measurements, obtained either from profiles or sub-surface measurements at fixed depth

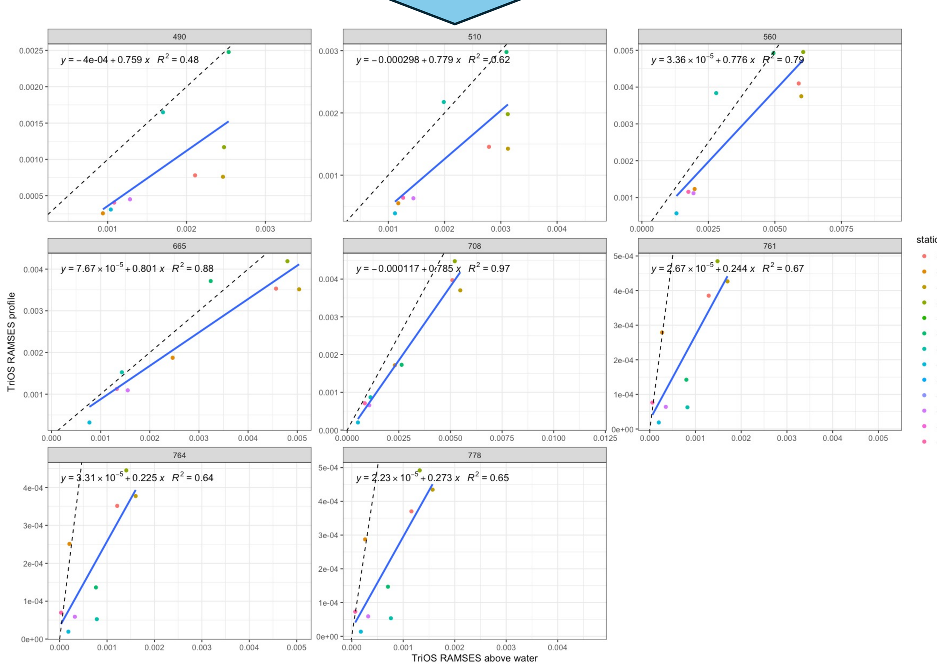

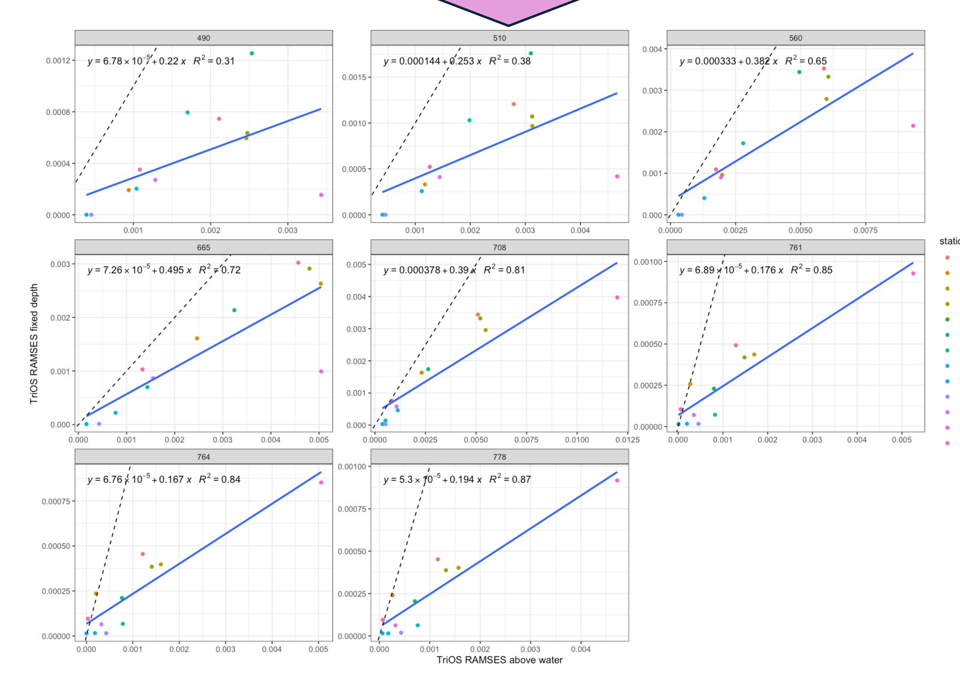

Comparison of above and in-water radiometric measurements at study site #4349

Measurements were performed under variable environmental conditions, resulting in variability in the derived $R_{rs}(\lambda)$. Both below-water measurements also show considerably lower values, potentially due to shading from the platform.

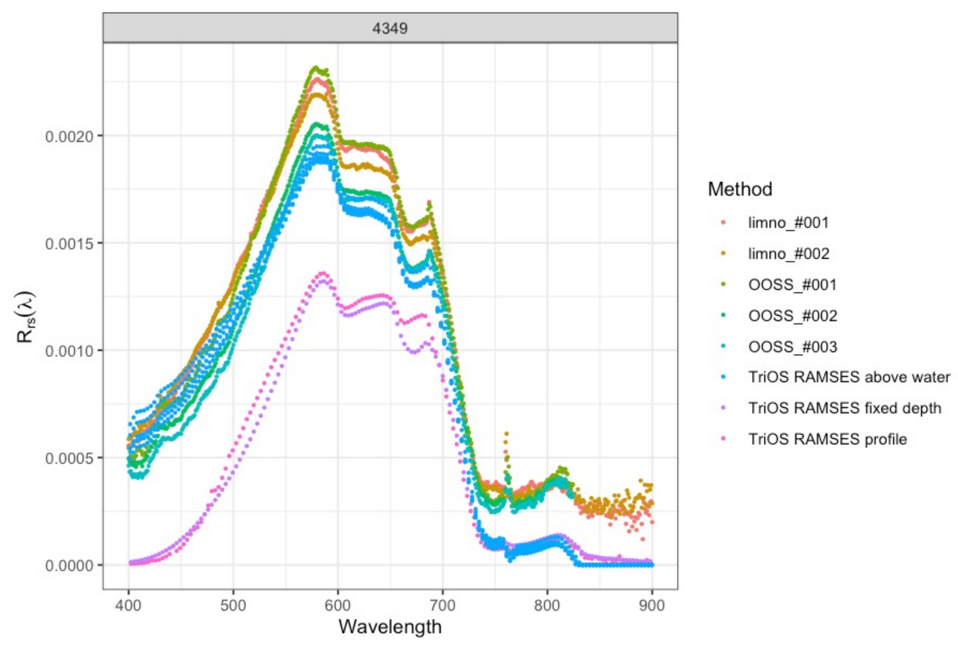

Conclusions

- Measurements were performed under variable conditions.
- The agreement between above-water and below-water measurements was better:
  - under moderate conditions: Chl < 4 µg/L, TSM < 6 mg/L, $a_{CDOM}(440)$< 2.1m^{-1}
  - when $R_{rs}(\lambda)$ was derived from profile measurements.
- Under highly absorbing and eutrophic conditions, the radiometers' responsivity limits the possibility of profile measurements.
- Repeated measurements would increase confidence in the below-water measurements.

Acknowledgements: Estonian Research Council grant PRG2646 "Methods, Traceability and Validation of the In-Water Ocean Color Measurements". ESA Estonia research infrastructure funded by the Estonian Research Council grant TARISTU24-TK3. FRM4SOC Phase-2 – EUMETSAT project no. EUM/CO/21/460002539/JIG